Supplementary Information for Facets of the Tropical High-Cloud Feedback in a Global Storm-Resolving Model

Jakob Deutloff[1, 2, 3*], Stefan A. Buehler[1, 2], Julia Windmiller[4, 5], Ann Kristin Naumann[6]

[1*]Earth System Sciences, Atmospheric Science, University of Hamburg, Hamburg, Germany.
[2]Earth and Society Research Hub (ESRAH), Hamburg, Germany.
[3]International Max Planck Research School on Earth System Modelling (IMPRS-ESM), Hamburg, Germany.
[4]Max Planck Institute for Meteorology, Hamburg, Germany.
[5]Monash University, Melbourne, Australia.
[6]Ludwig-Maximilians-Universität in Munich, Munich, Germany.

*Corresponding author(s). E-mail(s): jakob.deutloff@uni-hamburg.de;
Contributing authors: stefan.buehler@uni-hamburg.de; julia.windmiller@mpimet.mpg.de; a.naumann@lmu.de;

S1 Influence of Time of Occurrence on High-Cloud Radiative Effect

The SW $C(I)$ becomes stronger for more incoming solar radiation, which can be modulated by the local time at which the respective cloud occurs, and its distance to the equator. To first order, the incoming SW radiation is governed by the timing of the clouds. This becomes evident by the solar radiation closely following the time difference to noon (Fig. S1).

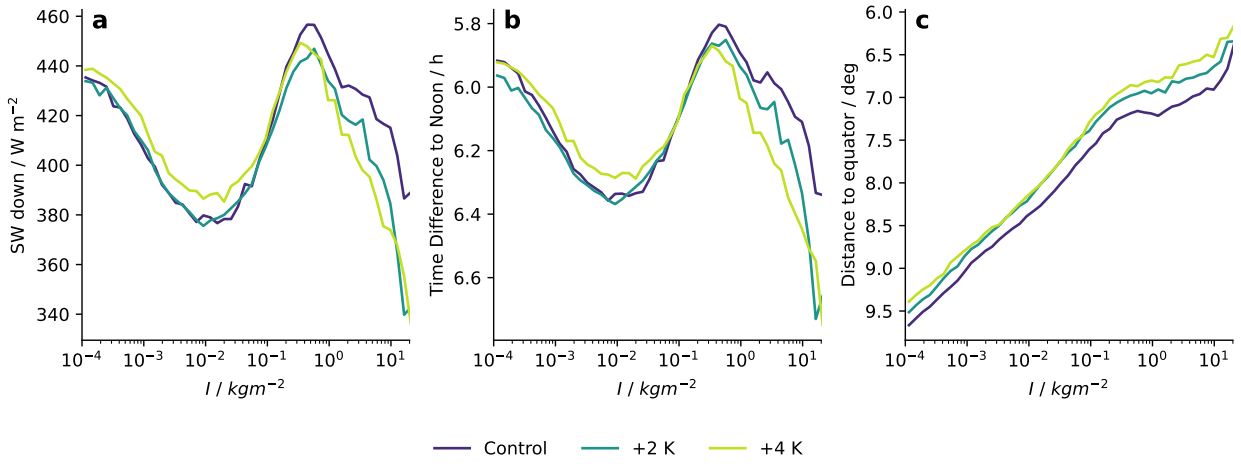

Fig. S1 (**a**) Incoming SW radiation, (**b**) time difference to noon and (**c**) distance to the equator binned by ice water path (I).

S2 Congestus Feedback

Liquid clouds can either be part of a high cloud if the frozen and liquid condensate sufficiently overlap, or not (Eq. 3). At low I, overlap between frozen and liquid clouds is rare, but it exists. We refer to such overlapping clouds as congestus clouds, since they typically contain more liquid than frozen condensate. The rest of the liquid clouds are referred to as low clouds.

Liquid clouds reduce as surface temperature increases (Fig. S2a), which causes a reduction in both low clouds (Fig. S2b) and congestus clouds (Fig. S2c). Congestus clouds also carry less liquid as surface temperatures increase. The median liquid water path of congestus clouds at $I < 10^{-1}$ kg m^{-2} is 0.169 kg m^{-2} (control), 0.152 kg m^{-2} (+2 K) and 0.145 kg m^{-2} (+4 K).

The reduction of congestus clouds together with their reduced amount of liquid condensate causes the SW $C(I)$ to become less negative at $I < 10^{-1}$ kg m^{-2} in response to surface warming (Fig. 1d). This becomes apparent when we calculate $\Delta C_{\mathrm{SW}}(I)$ only for frozen clouds, i.e. liquid condensate is not included as part of the high clouds. In this case, the positive $\Delta C_{\mathrm{SW}}(I)$ at $I < 10^{-1}$ kg m^{-2} does not exist (Fig. S3).

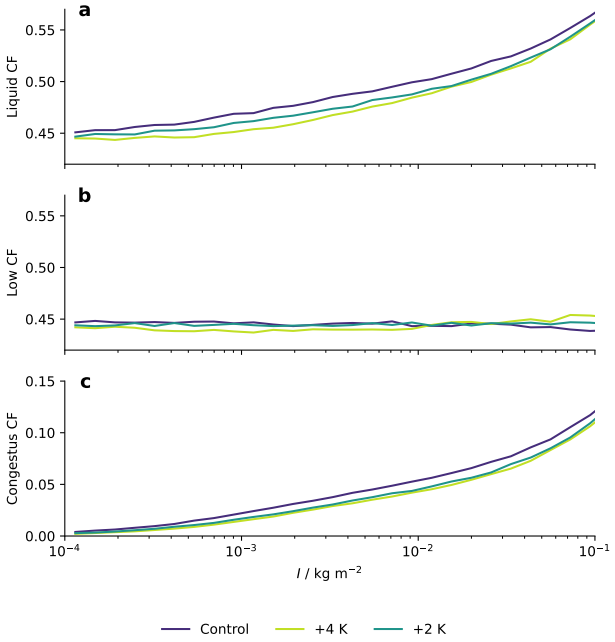

Fig. S2 (**a**) Fraction of all liquid clouds, (**b**) fraction of low clouds (liquid clouds that are not part of the high clouds) and (**c**) fraction of congestus clouds (liquid clouds that are part of the high clouds).

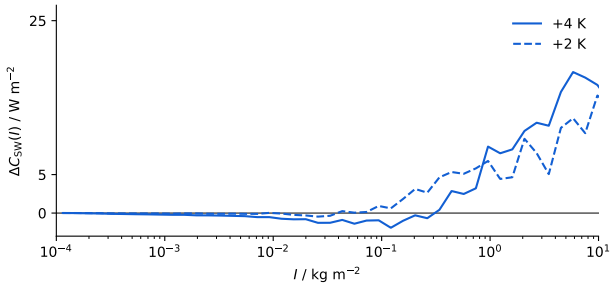

Fig. S3 Change in the SW $C(I)$ for frozen clouds only.

S3 Albedo and Emissivity of High Clouds

We test whether changes in the microphysics of high clouds in response to surface warming alter the high-cloud opacity by calculating the high-cloud albedo and emissivity [1]. Both the albedo and the emissivity of high clouds remain remarkably constant despite surface warming (Fig. S4). We conclude from this that potential changes in the microphysics of high clouds in response to surface warming do not alter their opacity in our simulations.

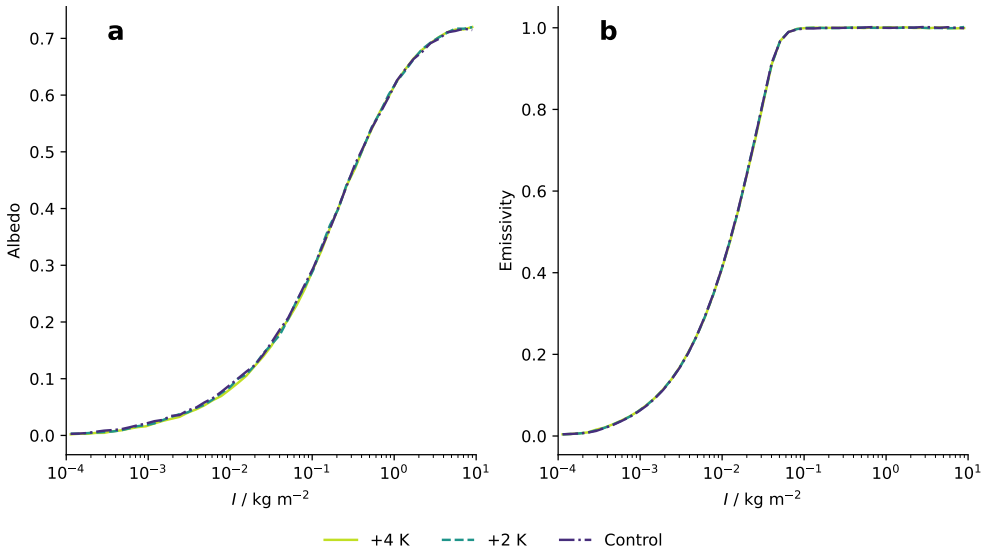

Fig. S4 (**a**) Albedo of high clouds and (**b**) emissivity of high clouds.

S4 Constant Ozone Simulation

The temperature profile of the +4 K warming simulation with prescribed constant ozone simulation shows clear tropopause warming. This is not the case for warming simulations with interactive ozone, for which the temperature profile shifts upward.

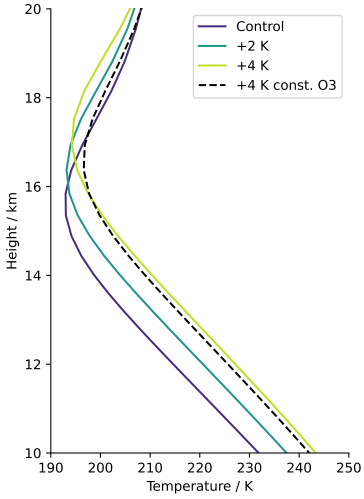

Fig. S5 Mean clear-sky temperature profiles.

S5 Stability Iris

The static stability is increasing with surface warming as expected (Fig. S6b); however, this is partly cancelled by an increase in clear-sky radiative cooling (Fig. S6a). Therefore, changes in the subsidence profiles and the convergence are small (Fig. S6c, d). This cancellation was also found by previous studies, but seems more pronounced in our simulations [2].

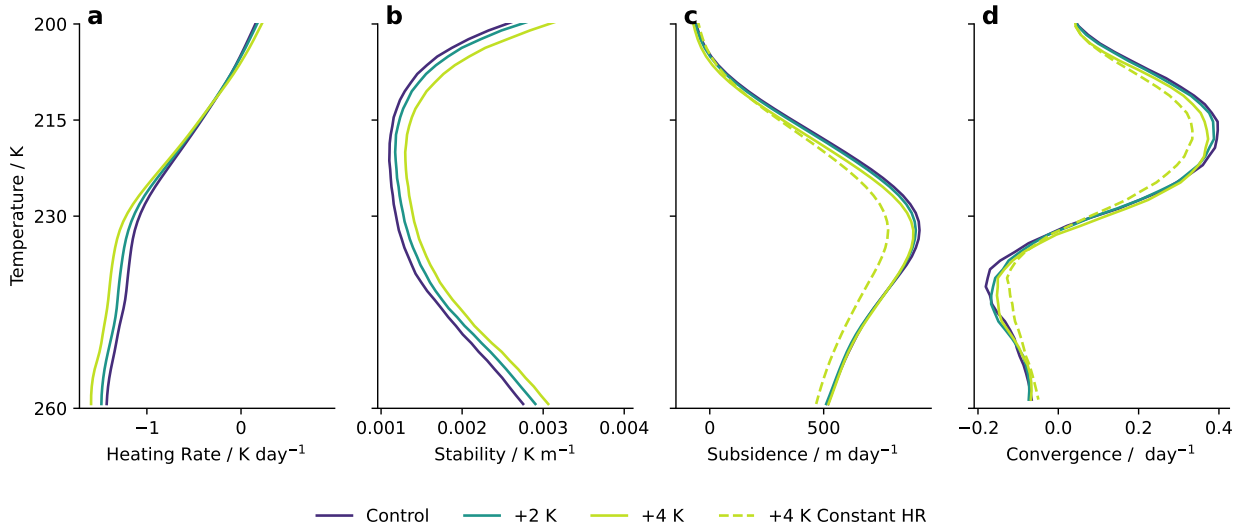

Fig. S6 (**a**) Mean profiles within the clear-sky atmosphere of heating rate, (**b**) static stability, (**c**) radiatively driven subsidence and (**d**) horizontal convergence of radiatively driven subsidence. The dotted line in **c** and **d** shows results for the +4 K simulation with the heating rate fixed at the control profile.

Regressing the maximum clear-sky convergence ($D_{\max}$) against the surface temperature anomaly yields the decrease of $D_{\max}$ in response to increasing surface temperatures, which is central to the stability iris theory (Fig. S7).

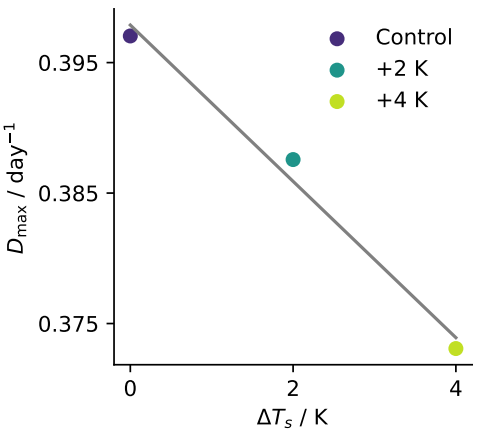

Fig. S7 Maximum clear-sky convergence ($D_{\max}$) plotted against the surface temperature anomaly (ΔT_s) and linear regression of the data (grey line).

S6 Heating Rates

Radiative heating rates (Q) are calculated as

$$Q = \frac{1}{\rho c_\mathrm{p}} \frac{\mathrm{d}F}{\mathrm{d}z},$$

where ρ is air density, c_p specific heat capacity of air and F the radiative flux. As the surface warms, the atmosphere expands, and isotherms move to lower pressure and hence lower density. The high clouds follow the isotherms [3], and hence also move to lower density. The flux divergence $\frac{\mathrm{d}F}{\mathrm{d}z}$ is expected to stay constant at a given isotherm, despite the isothermal expansion of the atmosphere [4]. The decrease in density at cloud height should therefore imply a higher magnitude of cloud radiative heating [5]. However, changes in the diurnal cycle of clouds will affect the SW $\frac{\mathrm{d}F}{\mathrm{d}z}$. We test the relative importance of the density effect and the change in flux divergence for the overall change in heating rates by decomposing the change in heating rates:

$$\Delta Q = \underbrace{\Delta \frac{1}{\rho c_\mathrm{p}} \frac{\mathrm{d}F}{\mathrm{d}z}}_{\text{Density}} + \underbrace{\frac{1}{\rho c_\mathrm{p}} \Delta \frac{\mathrm{d}F}{\mathrm{d}z}}_{\text{Flux Divergence}} + \underbrace{\Delta \frac{1}{\rho c_\mathrm{p}} \Delta \frac{\mathrm{d}F}{\mathrm{d}z}}_{\text{non-linear}}.$$

This decomposition reveals that the decrease in density is the main driver for changes in heating rates (Fig. S8). Changes in the flux divergence exist and cause changes in radiative heating, but they are noisier and contribute less to the overall change in radiative heating.

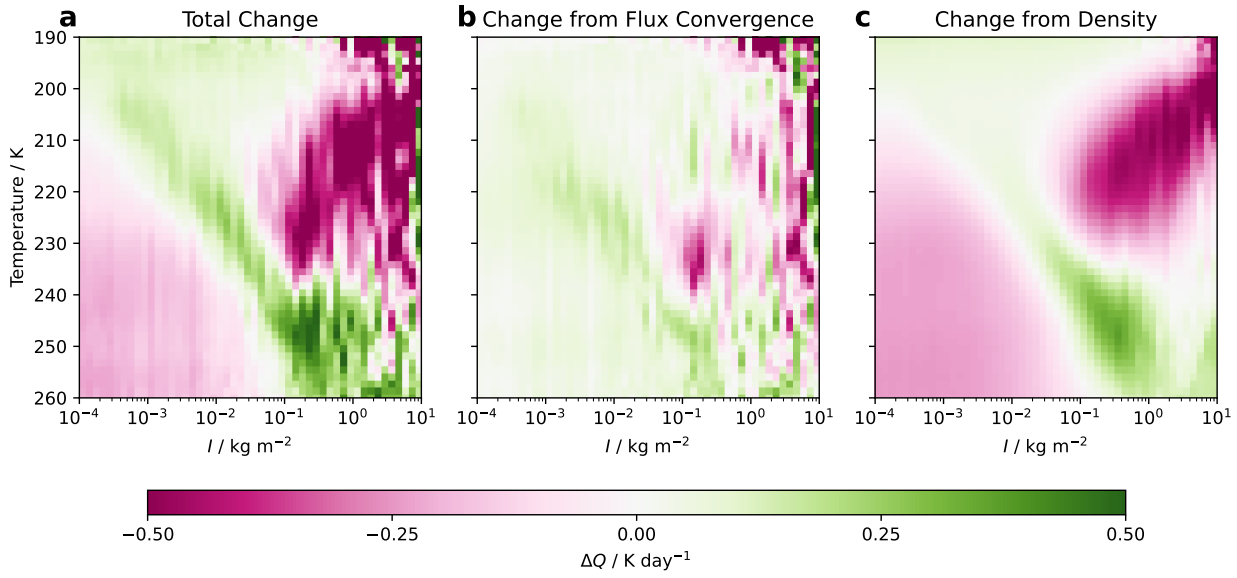

Fig. S8 (**a**) Change in cloud radiative heating for the +4 K simulation and the decomposition of the change in heating rate into contributions from (**b**) the change in flux convergence and (**c**) the change in density.

S7 Testing Convergence of Statistics

To test whether three months of simulation are long enough to reach a statistically stable state, we investigate the most fragile quantity of our analysis, ΔP. When plotted with data from the first month, the first two months and all three months of simulation, ΔP shows convergence (Fig. S9). This proves that three months of simulation are sufficient to reach a statistically stable state.

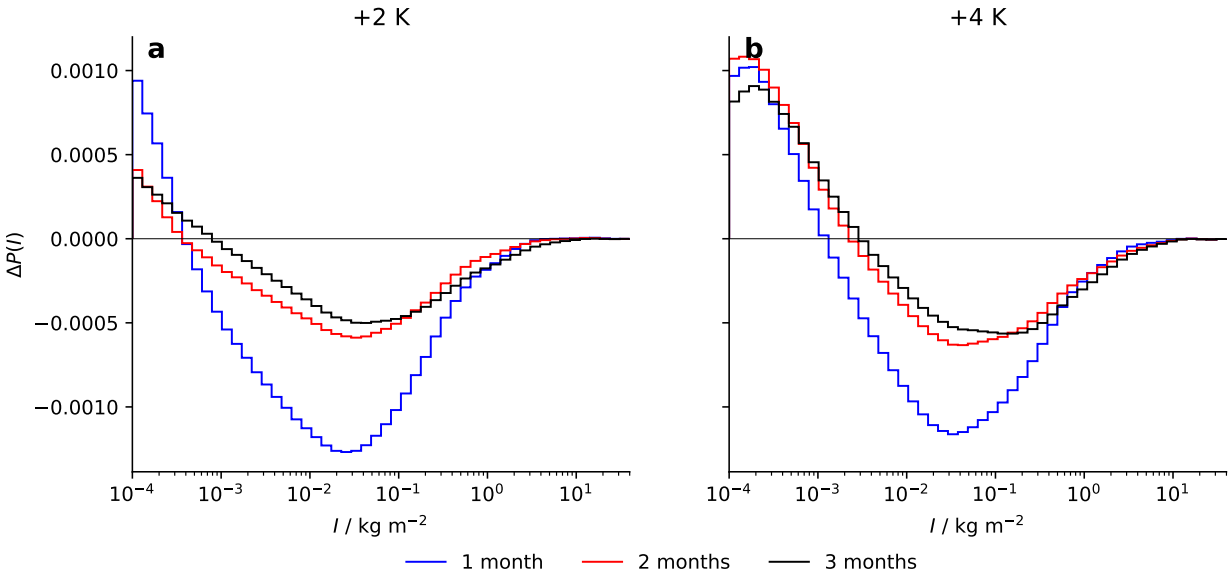

Fig. S9 The difference between the ice water path frequency with respect to the control simulation ($\Delta P(I)$) based on data from the first month, the first two months and all three months of the simulations for (**a**) the +2 K and (**b**) the +4 K simulation.

S8 Sensitivity to Connectedness of Liquid and Frozen Clouds

Varying the threshold used to decide whether liquid clouds are part of the high, frozen cloud above mostly affects our estimate of the SW F_C (Fig. S10). This is explained by the SW C of liquid clouds being much stronger than their LW C [1]. In the paper, we use 5% as the threshold for connectedness.

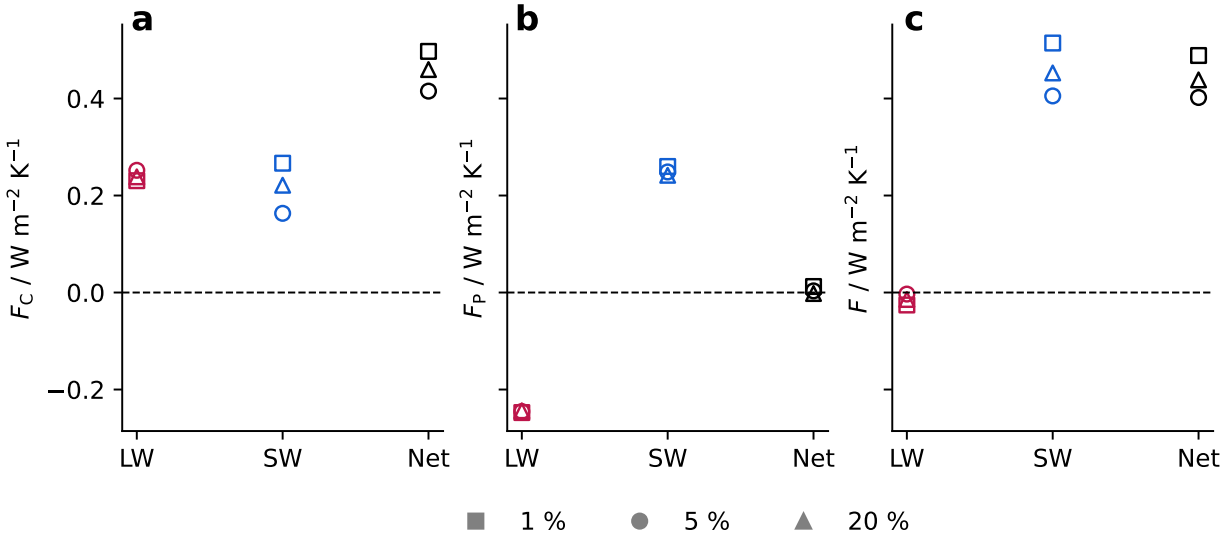

Fig. S10 High-cloud feedback from the +4 K simulations for different thresholds in the calculation of connectedness. (**a**) Feedback from changes in $C(I)$, (**b**) feedback from changes in $P(I)$ and (**c**) total feedback.

S9 Liquid Clouds at the Transition to Deep Convection

Liquid clouds are typically not connected to the frozen clouds at low I, but become increasingly connected towards high I. According to our definition of high clouds, liquid clouds are part of the high clouds if the liquid and frozen condensate within a column sufficiently overlap (Eq. 3). The transition from liquid clouds being unconnected with the frozen clouds to liquid clouds being part of the high cloud occurs at 1 kg m^{-2} $< I <$ 10 kg m^{-2} (Fig. S11).

Without the tuning factor in Eq. 3, this transition would shift towards higher I with warming, which would make the SW $C(I)$ become less negative. This is a consequence of liquid clouds being more reflective than the ocean surface. We regard this change in the SW $C(I)$ and the associated feedback to be artificial since it depends on subtle details of our definition of high clouds. Therefore, we introduce the tuning factor to keep the liquid cloud fraction constant with warming.

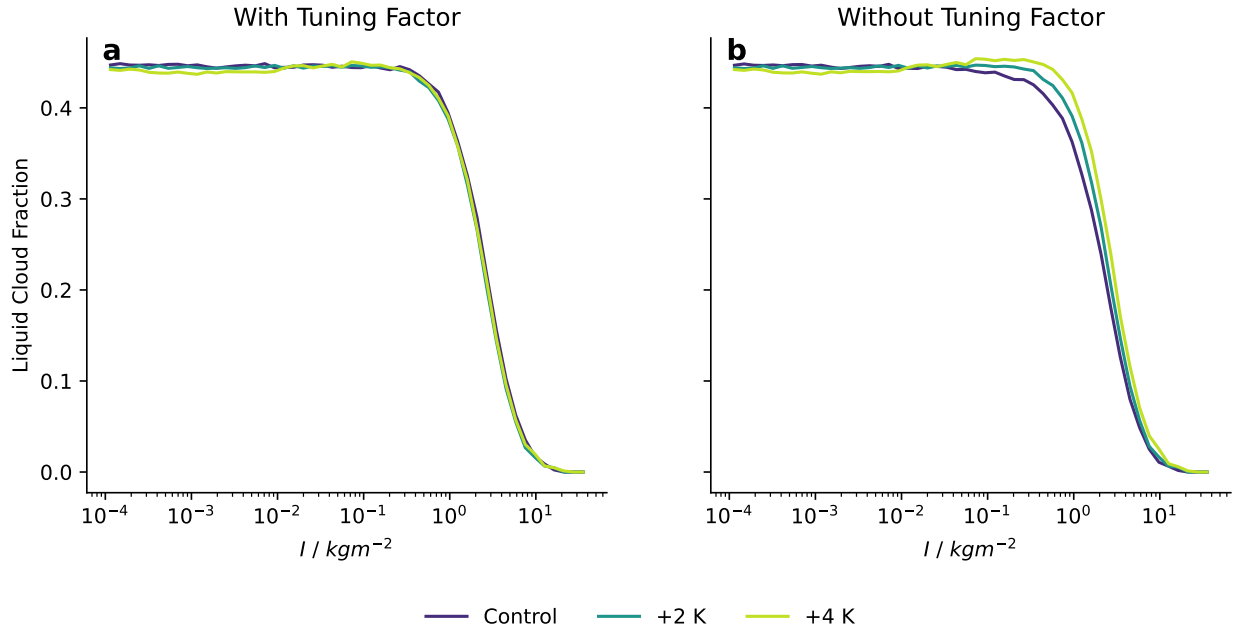

Fig. S11 Fraction of liquid clouds with a liquid water path of more than 10^{-4} kg m^{-2} that are not part of high clouds (**a**) with and (**b**) without including the tuning factor designed to keep the liquid cloud fraction constant with warming.

References

[1] Deutloff, J., Buehler, S.A., Brath, M., Naumann, A.K.: Insights on Tropical High-Cloud Radiative Effect From a New Conceptual Model. Journal of Advances in Modeling Earth Systems **17**(2), 2024–004615 (2025) https://doi.org/10.1029/2024MS004615 . _eprint: https://onlinelibrary.wiley.com/doi/pdf/10.1029/2024MS004615. Accessed 2025-03-03

[2] Bony, S., Stevens, B., Coppin, D., Becker, T., Reed, K.A., Voigt, A., Medeiros, B.: Thermodynamic control of anvil cloud amount. Proceedings of the National Academy of Sciences **113**(32), 8927–8932 (2016) https://doi.org/10.1073/pnas.1601472113 . Accessed 2023-06-01

[3] Hartmann, D.L., Larson, K.: An important constraint on tropical cloud - climate feedback. Geophysical Research Letters **29**(20), 12–1124 (2002) https://doi.org/10.1029/2002GL015835 . _eprint: https://onlinelibrary.wiley.com/doi/pdf/10.1029/2002GL015835. Accessed 2023-07-07

[4] Jeevanjee, N., Romps, D.M.: Mean precipitation change from a deepening troposphere. Proceedings of the National Academy of Sciences **115**(45), 11465–11470 (2018) https://doi.org/10.1073/pnas.1720683115 . Publisher: Proceedings of the National Academy of Sciences. Accessed 2025-03-25

[5] Gasparini, B., Mandorli, G., Stubenrauch, C., Voigt, A.: Basic Physics Predicts Stronger High Cloud Radiative Heating With Warming. Geophysical Research Letters **51**(24), 2024–111228 (2024) https://doi.org/10.1029/2024GL111228 . _eprint: https://onlinelibrary.wiley.com/doi/pdf/10.1029/2024GL111228. Accessed 2025-01-22